In Situ STM Imaging of Silicon(111) in HF under Potential Control

Shueh-Lin Yau, Fu-Ren F. Fan, and Allen J. Bard*

Department of Chemistry and Biochemistry, The University of Texas at Austin, Austin, Texas 78712

ABSTRACT

In situ scanning tunneling microscopy (STM) and atomic force microscopy (AFM) were employed to examine the surface morphology of a Si(111) cathode in 1% HF or a mixed HF and H_2O_2 solution under potential control. In the absence of H_2O_2, *in situ* STM revealed island-like features due to the native defects at the Si substrate and the subsequent dissolution of the native SiO_2 layer by the HF etchant. Atomic resolution was possible, and a well-ordered hexagonal array, presumably the Si(111)-(1 × 1):H phase, was imaged by STM after the oxide layer was removed. This long-range ordered structure was stable in dilute HF for *ca.* 1 h before it became disordered by the evolution of H_2. In a mixed solution of H_2O_2 and HF, depending on the relative concentration of these two species, either the oxide formation or its subsequent dissolution dominated. When the former reaction was more important, the STM tip physically scratched the insulating SiO_2 layer. At higher relative HF concentrations, a long-range ordered one-dimensional fiber structure arranged in a sawtooth pattern was imaged, when the dissolution of SiO_2 occurred. These surface features are attributed to chemical etching of Si, possibly the metastable SiOH surface species.

The study of the Si/HF interface is of both technological and academic interest. For example, treating Si with HF passivates the Si surface and produces one exhibiting an unusual surface-recombination velocity.[1] As indicated by the Fourier transform infrared spectroscopy (FTIR), electron energy loss spectroscopy (EELS), and scanning tunneling microscopy (STM), this treatment produces an atomically flat surface with less than a 5% defect density.[2,3] This type of surface pretreatment is important in the production of high quality Si semiconductors and the development of Si solar cells.[4] The proposed mechanism for Si surface passivation by HF involves dissolution of SiO_2 followed by termination of Si dangling bonds by hydrogen.[5] However, the mechanism of SiO_2 dissolution and the stability of the H-saturated Si surface toward air oxidation have still not been elucidated.[6,7] Trucks *et al.*[5] performed *ab initio* molecular-orbital calculations on the mechanism of formation of Si—H, while Judge[8] and Proksche *et al.*[9] conducted experiments to illustrate the dependence of the etching rate on the chemical nature of the etchant. Recently, the scanning probe microscopic techniques have allowed scientists to probe interfacial phenomena at the atomic level.[10] For example, although the H-terminated surface was claimed to be stable in air for several hours,[6] Becker *et al.*[3] used STM to demonstrate the reactivity of the HF-etched Si surface with contaminants.

In this study we examine the aqueous Si/HF interface and the nature of the surface after chemical dissolution of the native SiO_2 layer by *in situ* STM and AFM. The Si(111) surface has been extensively studied in ultrahigh vacuum (UHV) by STM,[11] but there have been few studies with the Si immersed in a liquid[12] and, to our knowledge, none that show high-resolution images of the surface of a Si electrode under potential control. STM has been employed to study semiconductor electrochemistry,[12] however, the resolution has been restricted to the micron or submicron range. In the present study, we report the surface morphology of an n-type Si(111) electrode immersed in a dilute HF solution and the first *in situ* STM atomic resolution images of a Si(111) electrode. We show that the dissolution of the oxide layer preferentially starts at defects such as the observed channels, and results in island-like surface features that are eventually replaced with an atomically flat surface. The *in situ* STM revealed a well-ordered hexagonal lattice that strongly resembles the Si(111)-(1 × 1):H phase reported earlier by STM and AFM imaging in UHV and air.[3,6] This structure was found to be stable in the dilute HF solution for about 1 h. While H_2O_2 and HF have been used extensively to clean Si wafers, the quality of the HF-etched Si surface is difficult to evaluate in air because of the eventual oxidation of Si in air. We adapted the *in situ* STM imaging approach to examine the chemical etching of Si by H_2O_2-HF mixtures and found that the nature of the Si surface depended on the relative concentration of the two species. The Si surface was either covered with oxide produced by H_2O_2 or freed of oxide by HF dissolution. In the former case the STM tip physically scratched the Si surface due to the presence of the nonconducting SiO_2 layer, and in the latter case the *in situ* STM showed the formation of a fiber structure that disappeared within 1 min. We also observed a sawtooth step configuration that we attribute to an intrinsic surface mis-orientation and preferred formation of (111) microfacets.[13] We were thus able to use STM to study the dynamics of the etching process at atomic or near-atomic resolution.

Experimental

Si(111) wafers (n-type, 1 cm Ω resistivity) were obtained from Texas Instruments Inc. (Dallas, TX) and were used without further polishing. The orientation and quality of the Si(111) wafers were verified by the Laue back diffraction technique. As received, the Si wafers have a native oxide layer about 1.5 nm thick and a surface contamination layer of carbonaceous material. The Si samples were first washed with Millipore water and methanol before STM imaging. The original Si surface was strongly hydrophobic, as expected for one with an SiO_2 layer. STM imaging of Si in air was hampered by the uppermost SiO_2 layer; even with high bias voltage (3 V) stable imaging could not be implemented. After etching with HF, a Si surface could be imaged with STM in air, but the time was limited to about 30 min, presumably due to the facile oxidation of Si in an ambient environment. Therefore, we have adapted AFM to examine a Si sample after etching with 1% HF, while *in situ* STM was used to monitor SiO_2 dissolution in 1% HF. As H_2O_2 is one of the important components in wafer cleaning solution, its effect on Si surface quality was evaluated with STM in 1% HF after a Si sample was rinsed with a mixed solution of 1% HF and 2% H_2O_2 (by volume). Ultrapure HF and H_2O_2 solutions were obtained from Johnson-Matthey Inc. (Ward Hill, MA). A mixed solution of HF and H_2O_2 (1:2) was used to remove the carbonaceous contamination from the Si surface before imaging. The long-range ordered adlattice could be obtained on a Si(111) wafer immersed in a dilute HF solution only after it was cleaned with the HF-H_2O_2 solution. Thorough cleaning and etching was important in obtaining an atomically flat Si surface.

The STM and AFM were Nanoscope II instruments (Digital Instruments Inc., Santa Barbara, CA). The *in situ* STM electrochemical cell was of the same design as previously described.[10] The Si sample was clamped to the bottom of the cell by a 1 cm diam O-ring. Ohmic contact was made to

* Electrochemical Society Life Member.

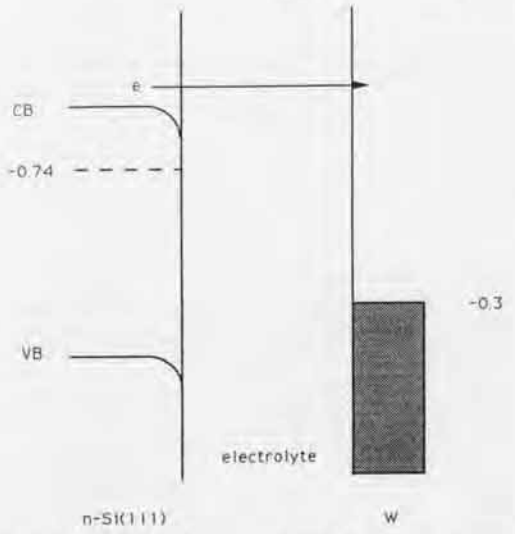

Fig. 1. Schematic band diagram of the Si-tip tunneling gap in dilute HF solution. Because the Si electrode was held at a potential (–0.95 V) more negative than its flatband potential (–0.74 V), an accumulation layer was created which enabled electron tunneling from the Si sample to the W tip (–0.35 V) in dilute aqueous HF solution.

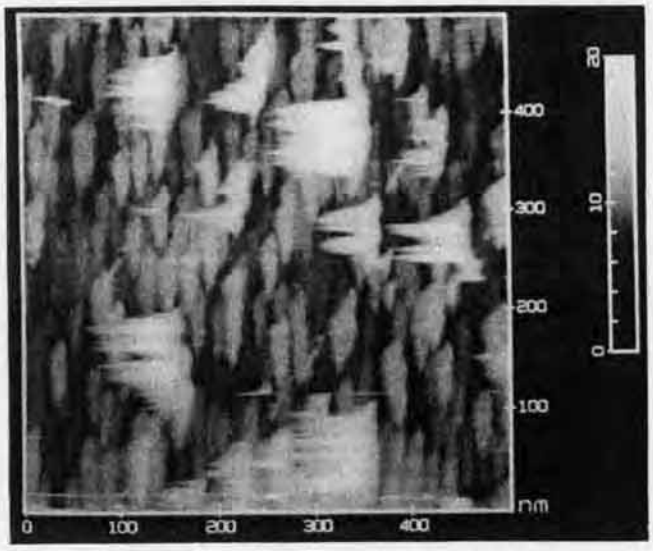

Fig. 2. Topographic *in situ* STM image of a Si(111) wafer immersed in 1% HF solution. The image was obtained with a 15 nA feedback current at E_{Si} = 0.95 V and E_{tip} = –0.30 V. Most of the surface was covered with a thin layer of SiO_2 which did not significantly affect tunneling. However, a much thicker oxide layer in some regions probably caused physical contact between the tip and the SiO_2 layer.

the Si by GaIn alloy. The Pt counterelectrode and the Au quasi reference electrode were located at the inside perimeter of the O-ring. All the potentials reported here are referred to the normal hydrogen electrode (NHE) for convenience. The STM tips were prepared by electrochemical etching of a 0.010 in. W wire with 15 V ac in 1*M* KOH, followed by electrically insulating with colorless nail polish (Wet n' Wild, Pavion Ltd., Nyack, NY).[10] Although "good" tips are difficult to prepare reproducibly, about half of the nail polish-coated W tips were able to give atomic resolution. All the STM imaging experiments were performed under an Al cover in the dark. The AFM imaging in air of an HF-etched Si(111) wafer was conducted with a Nanoscope 100 μm cantilever (force constant = 0.58 N/m) with a Si_3N_4 tip. The force was approximately $10^{-8}N$ when the AFM was imaging. Reasonable resolution was obtained, as judged from the step edges.

Proper potential control of both the Si working electrode (E_{Si}) and the W tip electrode (E_{tip}) was required for successful *in situ* STM imaging, because the tip electrode was stable only within a certain potential window. Outside this window, the faradaic or charging current was too high to allow the proper operation of the STM feedback control. Furthermore, E_{tip} had to be more positive than E_{Si} so that electron tunneling from the conduction band of the Si to the W tip occurred (Fig. 1). As previously reported, when the tip was more negative than the working electrode, the strong electric field generated by the STM tip could lead to oxide formation which tends to destablize imaging.[12a] These are the main limitations for *in situ* STM in the study of electrochemical events. Moreover, because the tip was less than 1 nm away from the Si sample under imaging conditions, the tip electrode could interact with the Si sample as well as affect the concentration profiles of chemical species and the electric field distribution near the imaging area. For example, H_2 generated on the Si could be sensed by the tip electrode and resulted in a marked contribution of a faradaic component to the tip current.

Results and Discussion

In situ STM of Si(111) in 1% HF.—The Si flatband potential, E_{FB}, estimated from the potential for the onset of photocurrent on the n-Si electrode, was *ca.* –0.74 V in dilute HF solution. To achieve optimum STM resolution, the Si substrate was held at –0.95 V, which was more negative than E_{FB}; E_{tip} was fixed at –0.35 V. These experimental parameters were used in all of the *in situ* STM imaging experiments. The accumulation of electrons at the Si surface facilitates the electron flow from Si to the solution species or to the W tip (Fig. 1). A cathodic current of –4 μA/cm^2 passed through the Si electrode, indicating hydrogen evolution at the Si surface. Hydrogen bubbles emerged locally at the perimeter of the region of the Si sample confined by the 1 cm diam O-ring while the central part of the Si sample under STM imaging was basically quiescent. This uneven current distribution on the Si electrode could stem from the arrangement of the Pt counterelectrode near the outside of the Si electrode. The current density on the Si electrode will be higher at the regions closer to the Pt counterelectrode.

In situ STM was first used to examine the chemical dissolution of the native SiO_2 layer in 1% HF solution. Figure 2 shows the STM constant-current image of the Si(111) surface acquired immediately after 1% HF was added to the cell. Despite some thermal drift, *in situ* STM showed island features exhibiting average dimensions of *ca.* 80 nm long and 20 nm wide and 1.5 nm higher than their neighboring trenches. These surface features were stable in 1% HF, but less so in 5% HF which accelerated dissolution of the SiO_2. The island features in Fig. 2 represent partial dissolution of the native SiO_2 layer, the original morphology of which could be probed by AFM imaging in air (Fig. 3). These *in situ* STM results are similar to those of a previous STM and high resolution transmission electron microscope (HRTEM) study of SiO_2 by Carim *et al.*[13] who concluded that the STM probes the Si—SiO_2 interface rather than the oxide-vacuum boundary. Based on these results, we propose that the *in situ* STM was imaging a Si surface probably covered with a thin oxide layer. While most islands were well resolved by the STM, some portions of the surface exhibited poor resolution. These erratic z-excursions are tracking errors of the electrode which result from physical contact of tip and sample.

HF, HF_2^-, and polymeric $HF_x^{(x-1)-}$ are the principle chemical species which dissolve the SiO_2 layer, whose concentration in aqueous solution depends on the concentration of HF and the pH.[14] In dilute HF, HF_2^- is the major component and shows a four-fold higher etching rate than HF.[9] In concentrated HF solution, the polymeric phase dominates the etching reaction. The dissolution of SiO_2 can generally be written as

$$SiO_2 + 6HF \rightarrow SiF_6^{2-} + 2H^+ + 2H_2O \quad [1]$$

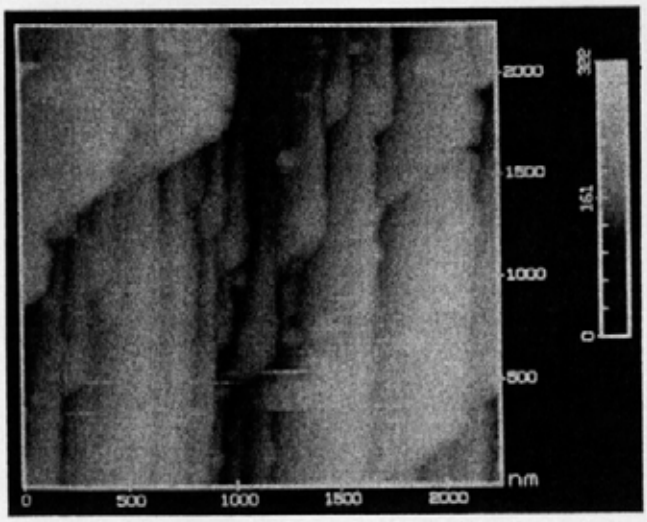

Fig. 3. AFM image of an HF-etched Si(111) surface. The image was obtained in constant force mode operating at approximately 10 nN. Island features are seen in this image and in Fig. 2, although they are different in size. The sparsely distributed lumps are probably the result of contamination.

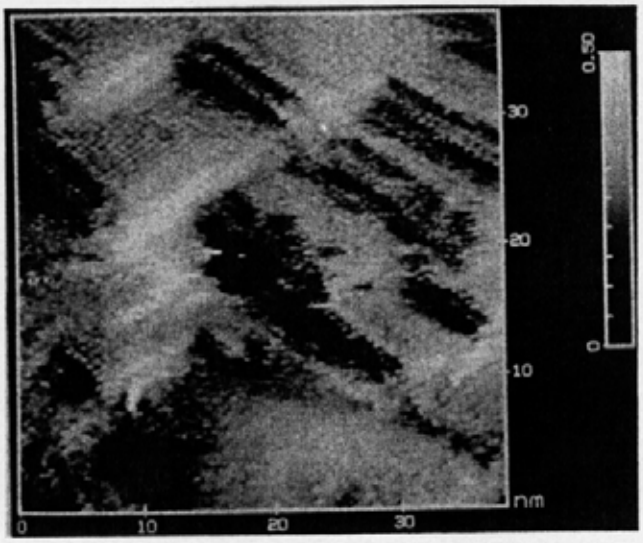

Fig. 4. *In situ* STM atomic resolution of hydrogen terminated Si(111) in 1% HF solution. The Si(111) sample was pretreated with alcohol and triply distilled water, followed by chemical etching in dilute H_2O_2 and HF before it was mounted in the STM cell. Thermal drift and error in the calibration of the piezo cause some distortion of the image. The potential of Si and the W tip were −0.95 and −0.35 V, respectively.

After the amorphous SiO_2 layer is removed, the uppermost layer of Si atoms finally dissolves as SiF_4 after progressively reacting with HF, and the second layer of Si atoms is saturated with H atoms, as described by Truck *et al.*[5] The H-terminated Si surface is stable toward further attack by HF. Formation of Si—F bonds by reaction of HF with Si—H does not occur because of the high activation barrier for the reaction of Si—H and HF, even though thermodynamic considerations would favor end-capping of the Si dangling bonds with F atoms, given their higher bond energy with respect to Si—H (565 KJ/mol *vs.* 318 KJ/mol[15]) This monohydride phase was stable, if the potential was not sufficiently negative to cause hydrogen evolution; conversion of the monohydride phase to the di- (Si=H_2) or tri- (Si=H_3) hydride phase before H_2 evolution is unlikely. This conversion would require the breaking of the Si—Si bond(s), which seems unlikely under cathodic conditions or in the absence of an oxidant in the solution.

When a Si(111) wafer was further treated with a dilute solution of H_2O_2 and HF, its surface quality was significantly improved. This result is demonstrated by the *in situ* STM image (Fig. 4) obtained in 1% HF which was used to remove the oxide layer. Atomically flat terraces as wide as 10 to 15 nm are separated by monoatomic steps intersecting in a sawtooth pattern. This surface feature was also observed by Hessel *et al.*[16] who attributed a surface misorientation of the Si sample to the structures of the steps. In the present study, misorientation of the Si wafer was observed along the <100> direction as well as in the <110> direction. The surface processes that occured on the Si and the surface structure are apparently governed by its potential and any tip-surface interaction in the *in situ* STM experiments. Hydrogen adsorption to form a Si(111)-(1 × 1):H phase is most likely responsible for the long range structure seen in Fig. 3. Note that this (1 × 1):H structure is the most stable configuration for the chemisorbed H on Si(111), regardless of the original structure of the Si substrate (with or without reconstruction).[17] Atomic resolution is seen in these images (Fig. 5). The Si—Si spacing between the maxima in the corrugations, 0.45 nm, is about 20% larger than expected of the hexagonal Si(111) lattice. The distortion for the ideal hexagonal Si(111) substrate was due to thermal drift in the piezoelectric scanner during STM imaging, while the asymmetric shape of the tip was responsible for the spatial dependence of the resolution. We did not notice any structural change before this well-ordered (1 × 1):H phase disappeared. A more negative potential favored hydrogen evolution with the formation of a well-ordered monohydride phase at the onset of H_2 evolution. Electrons tunnel from occupied states of the Si sample into unoccupied states of the W tip. Theoretical calculations[18] suggest that there are no surface states on the Si—H surface within the bandgap so that tunneling only occurs from the conduction band.

In Situ STM of Si(111) in HF/H_2O_2 solution.—The STM images in Fig. 6a-d show the evolution of surface features at a single location during etching by a dilute solution of 1% HF and 3% H_2O_2 (by volume). The STM images were acquired consecutively every 20 s at $E_{Si} = -0.95$ V and $E_{tip} = -0.30$ V. A Si fibrous structure running diagonally in the constant height STM images was seen in the A and B regions in Fig. 6a to c. These fibrous structures lasted for about 1 min then suddenly disappeared in Fig. 6d. Each of these atomics wires was about 2 nm wide but higher resolu-

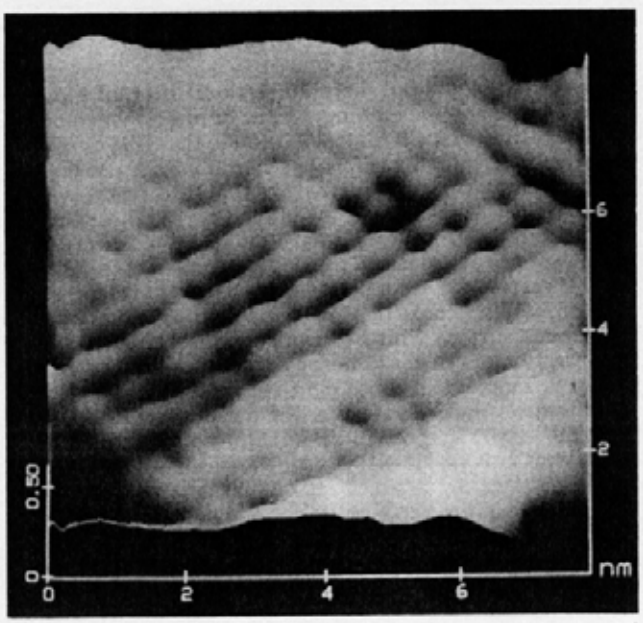

Fig. 5. Three-dimensional view of the atomic arrangement shown in Fig. 3. This image was subjected to a two-dimensional Fourier transform filter which removed high frequency noise equivalent to a distance below 0.30 nm.

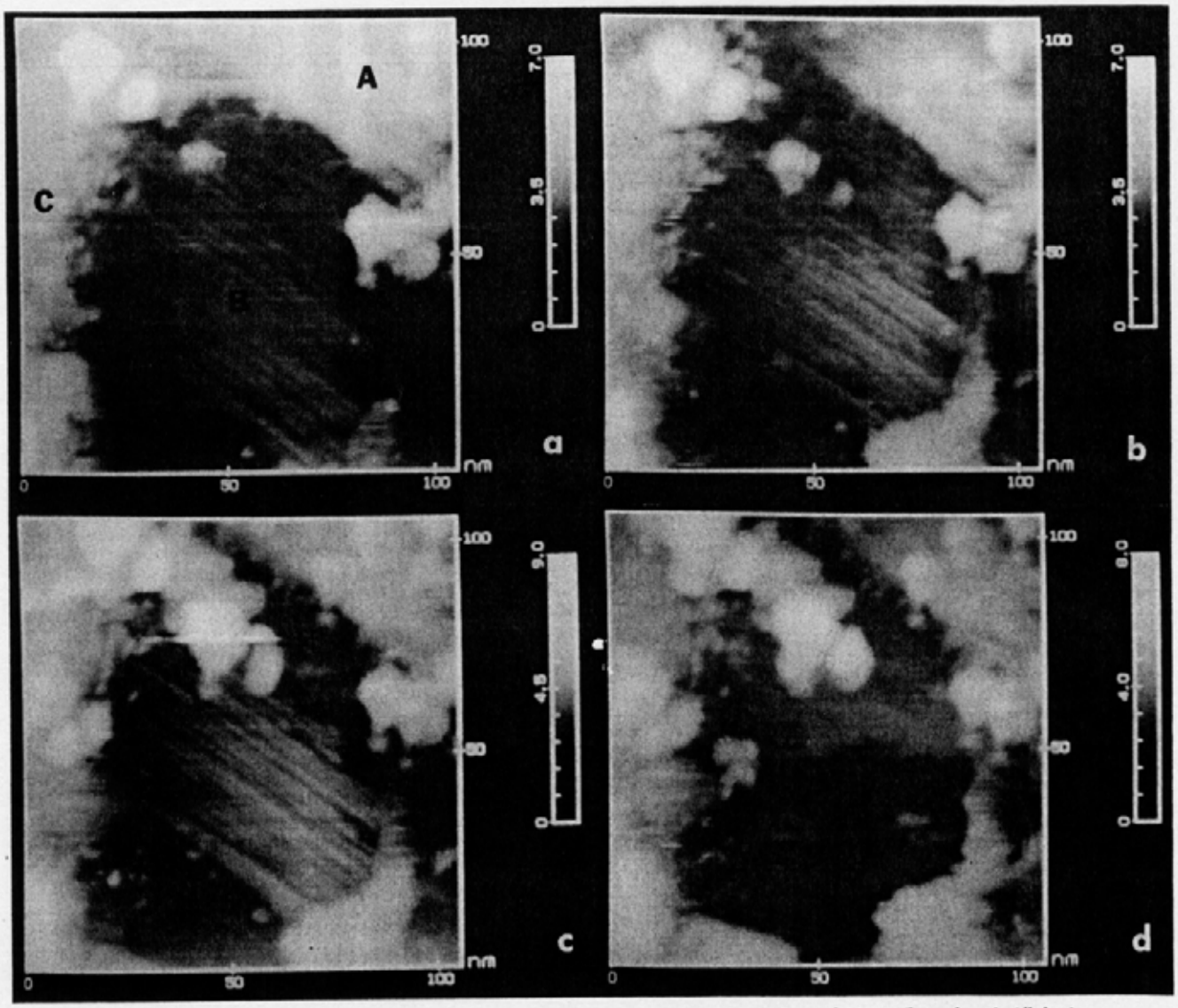

Fig. 6. A series of *in situ* STM images revealing wet chemical etching of Si in dilute 3% H_2O_2 and 1% HF (by volume). All the images were continuously collected every 20 s at E_s = −0.95 V and E_{tip} = −0.35 V, with a 5 nA tunneling current. Zones in the images are marked with A, B, C, and D for identification. The Si-fiber structure, clearly identified in region B from (a) to (c), suddenly disappeared in (d). Lumps of unknown composition gradually grew toward the fibers.

tion scans still could not distinguish their internal atomic structures. During the etching, lumps of unknown composition deposited in the B region. Although the STM does not reliably measure depths in *in situ* experiments, these lumps are apparently very conductive so that the tip was not driven to the Si substrate as it scanned across these areas. An island in the D region also gradually grew toward the fibers. We have also noticed the dependence of etch rate on the STM scan size. Larger scan sizes resulted in higher etch rates, probably because of a smaller shielding effect by the tip on the Si surface. This model also implies that the local concentration of reactants in the area being imaged could be very different from those in other areas.

To interpret the STM results, the dissolution of WO_3 by HF at the very end of the W tip must be considered, as the HF etchant can react with WO_3 to produce WF_6 ($WO_3 + 6HF \rightarrow WF_6 + H_2O$).[19] Hydrolysis of WF_6 generates HF and WO_4^{2-} which can form polyanions or heteropolyanions with the SiO_4^{4-} and precipitate on the Si cathode. This or perhaps contaminants, such as Cu^{2+} and Pb^{2+} which codeposit with W from the HF solution, are possible origins for the unknown clusters. The change of the tip shape could drastically change the STM resolution and was partly responsible for the sudden loss of the fibrous structures, although additional etching of Si might also occur. Growth of oxide was probably responsible for the surface change in the D region. Nevertheless, the oxide layer was so thin that the tunneling process was not inhibited. The following reaction mechanism is proposed to account for the *in situ* STM results in the HF-H_2O_2 mixture

$$(\equiv Si{-}H + H_2O_2 \rightarrow \equiv Si{-}OH_{(s)} + H_2O \quad [2]$$

$$(\equiv Si{-}OH_{(s)} + HF \rightarrow \equiv Si{-}F_{(s)} + H_2O \quad [3]$$

A H-terminated Si surface is generated after the dissolution of the SiO_2 layer. In the presence of H_2O_2, the Si—H bond is oxidized to Si—OH, as shown in Eq. 2. [The subscript (s) represents a surface species.] This reaction might be a two-step process as suggested by others.[20] The Si—OH bond is then preferentially attacked by HF to give Si—F. Further reactions to form the polyfluorinated Si center then occur before the Si atom finally leaves the surface as SiF_4 or SiF_6^{2-}. The rate of the reaction between SiF_{4-x} ($0 < x < 4$) and HF probably increases as more F atoms are bonded to the Si atoms because of the enhanced polarity of the Si reaction center as more F atoms are attached to it. The STM probably images the $Si{-}OH_{(s)}$ species, because the etch rate is controlled by reaction.[3]

Conclusions

We have used STM imaging to probe the dissolution process of the native SiO_2 layer and also to achieve *in situ* STM

atomic resolution of the Si(111)-(1 × 1):H phase in a dilute HF solution under potential control. This *in situ* STM approach is advantageous in terms of examining the surface states or defects which may be buried under the inevitable oxide layer under ambient conditions. The hydrogen passivated Si surface was sufficiently stable toward attack by H_2O, HF, and dissolved O_2 for about 1 h before hydrogen evolution occurred on the Si surface and surface roughening began. Furthermore, *in situ* STM indicated that chemical etching of Si in HF occurs in the presence of H_2O_2 even under cathodic conditions. Etching caused formation of a sawtooth pattern, attributed to an anisotropic etching reaction and surface defects.

Acknowledgments

The support of this research by a grant from the Office of Naval Research and the National Science Foundation (CH 911 9851) is gratefully acknowledged.

Manuscript submitted April 9, 1992; revised manuscript received July 1, 1992.

The University of Texas assisted in meeting the publication costs of this article.

REFERENCES

1. E. Yablonovitch, D. L. Allara, C. C. Chang, T. Gmitter, and T. B. Bright, *Phys. Rev. Lett.*, **57**, 249 (1986).
2. P. Dumas and Y. J. Chabal, *Chem. Phys. Lett.*, **181**, 537 (1991).
3. R. S. Becker, G. S. Higashi, Y. J. Chabal, and A. J. Becker, *Phys. Rev. Lett.*, **65**, 1917 (1990).
4. S. M. Sze, *Semiconductor Devices: Physics and Technology*, John Wiley & Sons, Inc., New York (1985).
5. G. W. Trucks, K. Raghavachari, G. S. Higashi, and Y. J. Chabal, *Phys. Rev. Lett.*, **65**, 504 (1990).
6. Y. Kim and C. M. Lieber, *J. Am. Chem. Soc.*, **113**, 2335 (1991).
7. E. Sacher and A. Yelon, *Phys. Rev. Lett.*, **66**, 1647 (1991).
8. J. S. Judge, *This Journal*, **118**, 1772 (1971).
9. H. Proksche, G. Nagorsen, and D. Ross, *ibid.*, **139**, 521 (1992).
10. (a) A. A. Gewirth and A. J. Bard, *J. Phys. Chem.*, **92**, 5563 (1988); (b) S. L. Yau, X. P. Gao, S. C. Chang, B. C. Schardt, and M. J. Weaver, *J. Am. Chem. Soc.*, **113**, 6049 (1991); (c) S. L. Yau, C. M. Vitus, and B. C. Schardt, *ibid.*, **112**, 3677 (1990); (d) X. P. Gao, A. Hamelin, and M. J. Weaver, *Phys. Rev. Lett.*, **67**, 618 (1991).
11. (a) R. M. Tromp, R. T. Hamer, and J. E. Demuth, *ibid.*, **55**, 1303 (1985); (b) J. A. Stroscio, R. M. Feenstra, and A. P. Fein, *ibid.*, **57**, 2579 (1986); (c) J. J. Boland, *ibid.*, **65**, 3325 (1990).
12. (a) L. A. Nagahara, T. Thundat, and S. M. Lindsay, *Appl. Phys. Lett.*, **57**, 270 (1990); (b) P. Carlsson, B. Holmstrom, H. Kita, and K. Uosaki, *J. Electroanal. Chem.*, **283**, 425 (1990); (c) M. Szklarczk, A. Gonzalez-Martin, and J. O'M. Bockris, *Surf. Sci.*, **257**, 307 (1991).
13. A. H. Carim, M. M. Dovek, C. F. Quate, R. Sinclair, and C. Vorst,, *Science*, **237**, 630 (1987).
14. H. H. Broene and T. De Vries, *This Journal*, **69**, 1644 (1947).
15. J. Huheey, *Inorganic Chemistry; Principles of Structures and Reactivity*, 3rd ed, Harper & Row, New York (1983).
16. H. E. Hessel, A. Feltz, M. Reiter, U. Memmert, and R. J. Behm, *Chem. Phys. Lett.*, **186**, 275 (1991).
17. (a) T. Sakurai and H. D. Hgstrum, *Phys. Rev. B.*, **12**, 5439 (1975); (b) H. Fritzheim, H. Ibach, and S. Lehwald, *Phys. Lett. A*, **55**, 247 (1975).
18. J. A. Appalbaum and D. R. Hamann, *Phys. Rev. Lett.*, **31**, 106 (1973).
19. J. D. Lee, *Concise Inorganic Chemistry*, 4th ed., p. 720, Chapman & Hall, New York (1991).
20. J. E. A. M. van den Meerakker, *Electrochim. Acta.*, **35**, 1267 (1990).

Reprinted from JOURNAL OF THE ELECTROCHEMICAL SOCIETY
Vol. 139, No. 10, October 1992
Printed in U.S.A.